Anal Bioanal Chem (2011) 400:2475–2485
DOI 10.1007/s00216-010-4647-y

ORIGINAL PAPER

New fluorescent perylene bisimide indicators—a platform for broadband pH optodes

Daniel Aigner · Sergey M. Borisov · Ingo Klimant

Received: 15 October 2010 / Revised: 3 December 2010 / Accepted: 22 December 2010 / Published online: 22 January 2011

Abstract Asymmetric perylene bisimide (PBI) dyes are prepared and are shown to be suitable for the preparation of fluorescence chemosensors for pH. They carry one amino-functional substituent which introduces pH sensitivity via photoinduced electron transfer (PET) while the other one increases solubility. The luminescence quantum yields for the new indicators exceed 75% in the protonated form. The new indicators are non-covalently entrapped in polyurethane hydrogel D4 and poly(hydroxyalkylmethacrylates). Several PET functions including aliphatic and aromatic amino groups were successfully used to tune the dynamic range of the sensor. Because of their virtually identical spectral properties, various PBIs with selected PET functions can easily be integrated into a single sensor with enlarged dynamic range (over 4 pH units). PBIs with two different substitution patterns in the bay position are investigated and possess variable spectral properties. Compared with their tetrachloro analogues, tetra-*tert*-butyl-substituted PBIs yield more long-wave excitable sensors which feature excellent photostability. Cross-sensitivity to ionic strength was found to be negligible. The practical applicability of the sensors may be compromised by the long response times (especially in case of tetra-*tert*-butyl-substituted PBIs).

Published in the special issue *Analytical Sciences in Austria* with Guest Editors G. Allmaier, W. Buchberger and K. Francesconi.

Electronic supplementary material The online version of this article (doi:10.1007/s00216-010-4647-y) contains supplementary material, which is available to authorized users.

D. Aigner · S. M. Borisov (✉) · I. Klimant
Institute of Analytical Chemistry and Food Chemistry,
Graz University of Technology,
Stremayrgasse 9,
8010 Graz, Austria
e-mail: sergey.borisov@tugraz.at

Keywords Perylene · pH · Sensor · Fluorescence · Photoinduced electron transfer

Introduction

Monitoring of pH is of vital importance in biotechnology, environmental analysis and marine science, as well as in medicine. Optical pH sensors based on fluorescence are attractive since continuous, real-time measurement can be performed in a virtually contactless way. Unlike electrochemical pH sensors, they are not subject to electromagnetic interferences and can feature higher sensitivity within their dynamic range. Although optical pH sensors show cross-sensitivity to ionic strength, this inconvenience has been overcome by employing a low-charged indicator dye embedded into an uncharged matrix [1]. Another drawback is their narrow dynamic range, compared with electrochemical sensors. Many fluorescence pH sensors that can be found in the literature are based on fluorescein derivatives [2, 3], 8-hydroxypyrene-1,3,6-trisulfonate (HPTS) and its derivatives [4–7] or benzo[g]xanthene dyes [8–11]. However, most of the above sensors suffer from several drawbacks. Particularly, fluoresceins are commonly known for their limited photostability, especially in case of 2′,7′-alkyl-substituted derivatives [1]. Since HPTS is a highly charged molecule the cross-sensitivity to ionic strength is very high. Its lipophilic derivatives overcome these drawbacks but possess limited brightness. Benzo[g]xanthene dyes are long-wave excitable (>600 nm) [12], but show moderate brightness and are prone to photobleaching [13]. The above-mentioned indicators possess considerably different spectral properties in the protonated and deprotonated state and therefore are limited to systems where a (de) protonizable function is located within the chromophore.

However, pH sensitivity can also be introduced over photoinduced electron transfer (PET; Fig. 1). This process involves a redox reaction between a chromophore in the excited state and another functionality that can be found within the same molecule or in its close vicinity but in most cases is not integrated into it [14]. As PET is usually fast and fully reversible, it essentially constitutes a quenching process. In most cases, the above-mentioned functionality is an amino group which is capable of quenching only in the non-protonated state so that pH sensitivity is found if the pH is close to the pK_a of the amino group. Various chromophores including polyaromatic hydrocarbons [15–19], coumarins [20] and particularly naphthalimides [21–24] have already been shown to be quenched via PET by aliphatic amines. Therefore, the field of available fluorescent pH indicators can be dramatically extended by attaching amino groups to not intrinsically pH-sensitive chromophores. Notably, PET has been widely used for the design of ion sensors [25–31]. An advantage of PET-based systems is their modularity [32], i.e. fluorophore and receptor can be selected independently to specifically design a fluorescent indicator. Spectral properties are determined by the chromophore, whereas proton affinity (i.e. pK_a) is much more specific for the amino function (fluorophore-spacer-receptor systems) [14]. Furthermore, an extension of the pH-sensitive range is much less complicated in the case of PET-based pH indicators since several dyes with different pK_a values but virtually identical spectral properties can be combined. The drawbacks of the chromophores commonly used to design PET-sensors include their short-wave excitation (resulting in higher levels of auto-fluorescence in biological media and stronger light scattering) and, particularly, moderate to low luminescence brightness (BS, defined as the product of molar absorption coefficient ε and luminescence quantum yield QY). For example, the BS for naphthalimide-based indicators is ~12,000.

Perylene bisimide (PBI) dyes are known for their relatively high molar absorption coefficients 30,000–90,000 cm^{-1} M^{-1} [33, 34], fluorescence quantum yields close to unity [35], and excellent photostability [36]. These features enable their application in OLEDs [37], photovoltaic cells [38], fluorescent solar collectors [35] and dye lasers [39], to state only a few. Furthermore, PBIs feature good versatility in respect to synthetic modification [40–48] which makes them promising candidates for the design of new PET pH indicators. In fact, the pH sensitivity of PBIs with amino-functional substituents in both imide positions has already been demonstrated by De Silva and co-workers [49]. The application of those dyes in polymeric matrices was very limited due to their low solubility and high tendency to aggregation. Recently, Langhals and Pust [50] presented pH-sensitive nanomicells consisting of a PBI dye and sodium dodecyl sulphate. However, the field of perylene-based fluorescent pH indicators is still in its infancy. Here, we present a detailed study of various asymmetric PBI indicators that show appreciable pH sensitivity and bright fluorescence in different hydrogel matrices. As will be demonstrated, the pH sensitivity can be tuned by varying the amino functionality in the imide position whereas the substituents in the bay position influence the spectral properties.

Experimental

Materials

1,6,7,12-Tetrachloroperylene-3,4:9,10-tetracarboxylic bisanhydride and 1,6,7,12-tetra(4-*tert*-butylphenoxy)perylene-3,4:9,10-tetracarboxylic bisanhydride (technical grade) were purchased from Beijing Wenhaiyang Industry and Traiding Co. Ltd (http://china.zhaoteng.com). 1-*Methyl*-2-pyrrolidone and propionic acid were obtained from ABCR (www.abcr.de). All other solvents (synthesis grade) as well as NaCl and buffer salts were supplied by Carl Roth (www.roth.de). Deuterated chloroform $CDCl_3$ and anhydrous sodium sulphate were bought from Aldrich (www.sigmaaldrich.com). Silica gel (0.040–0.063 mm) was from Acros (www.fishersci.com). Polyurethane hydrogel (Hydromed™ D4) was purchased from CardioTech (www.cardiotech-inc.com). Poly (hydroxyproylmethacrylate) was obtained from Scientific

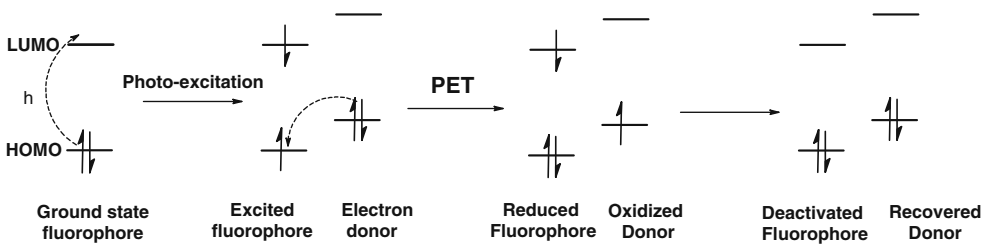

Fig. 1 Schematic layout of photoinduced electron transfer (*PET*) between an electron donor and a fluorophore (electron acceptor). As a result of excitation, a MO higher in energy becomes populated (i.e. the HOMO is elevated) and electron transfer becomes possible. If the donor is an amine, its HOMO is located at much lower energy in the protonated state so that PET becomes impossible

Polymer Products (www.scientificpolymer.com). Poly (hydroxyethylmethacrylate) (MW=150,000 g/mol) was from Polysciences Inc. (www.polysciences.com). Poly(ethylene glycol terephthalate) support (Mylar®) was from Goodfellow (www.goodfellow.com). Preparation of fluorescein octadecyl ester is reported elsewhere [1, 51]. 1,6,7,12-tetrachloro-*N,N'*-(2,6-diisopropylphenyl)perylene-3,4,9,10-tertracarboxylic bisimide was synthesized analogously to the literature procedure [33].

Syntheses

The synthetic concept is exemplified by the following synthesis of **2a**. The other dyes were obtained in a similar way. Their preparation is described in detail in the Electronic supplementary material.

1,6,7,12-Tetrachloro-N-(2,6-diisopropylphenyl)-N'-(3-morpholinopropyl)perylene-3,4:9,10-tertracarboxylic bisimide (***2a***). 1,6,7,12-Tetrachloroperylene-3,4:9,10-tetracarboxylic bisanhydride **1a** (1 g, 1.88 mmol) was dissolved in 1-*methyl*-2-pyrrolidone (NMP; 150 ml), warmed to 35 °C and a solution of 3-morpholinopropyl-1-amine (0.275 ml, 1.88 mmol) in NMP (20 ml) was added dropwise under vigorous stirring. The reaction progress was monitored via thin layer chromatography on silica gel and via UV-Vis spectroscopy. After TLC revealed total consumption of **1a** and no further shift in absorption spectra of the mixture was observed, propionic acid (50 ml) and 2,6-diisopropylaniline (1.54 ml, 7.51 mmol) were added. The mixture was heated to 130 °C for 21 h. After cooling to room temperature, it was poured onto 20% aqueous NaCl (1.4 l). The brown precipitate was separated by centrifugation, washed, redissolved in CH_2Cl_2, and dried with Na_2SO_4. Column chromatography with silica gel as the stationary and $CHCl_3$:MeOH as the mobile phase afforded 488 mg (32%) of **2a** as an orange powder. ^{1}H NMR (300 MHz, $CDCl_3$, TMS): δ=8.75 (2H, s, Cl–C–C<u>H</u>–(1)); 8.71 (2H, s, Cl–C–C<u>H</u>–(2)); 7.53 (1H, t, iPr–C–CHC<u>H</u>–, *J*=7.6 Hz); 7.37 (2H, *d*, iPr–C–C<u>H</u>–); 4.32 (2H, *t*, $(CO)_2NC\underline{H}_2$–, *J*=7.3 Hz); 3.63 (4H, *t*, $OC\underline{H}_2$–, *J*=4.5 Hz); 2.73 (2H, *m*, $PhC\underline{H}(CH_3)_2$, *J*=6.8 Hz); 2.53 (2H, *t*, $NC\underline{H}_2C_2H_5N(CO)_2$, *J*=6.9 Hz); 2.46 (4H, *t*, $NC\underline{H}_2CH_2O$, *J*=3.9 Hz); 1.96 (2H, p, $NCH_2C\underline{H}_2CH_2N$, *J*=7.3 Hz); 1.19 (12 H, dd, $-CH(C\underline{H}_3)_2$, J_1=6.7 Hz, J_2=4.1 Hz). Matrix-assisted laser desorption ionization-time of flight (MALDI-TOF): *m*/*z* [MH^+] 814.1382 found, 814.1409 calcd.

Preparation of the sensor foils

A "cocktail" containing indicator dye (0.44 mg), hydrogel D4/pHPMA (44 mg) and tetrahydrofurane (500 µl) was knife-coated on a dust-free Mylar support to obtain a ~7 µm thick sensing layer after solvent evaporation. For pHEMA, the cocktail consisted of 55 gl^{-1} polymer and 550 mg l^{-1} dye concentration in EtOH/H_2O (9:1 *v*/*v*).

Methods

Absorption measurements were performed on a Cary 50 UV-Vis spectrophotometer from Varian (www.varianinc.com). Fluorescence spectra were recorded on a Hitachi F-7000 spectrofluorimeter (www.hitachi.com). Relative fluorescence quantum yields were determined using rhodamine 101 (Fluka, www.sigmaaldrich.com) as a standard. NMR spectra were recorded on a 300 MHz instrument (Bruker) in $CDCl_3$ with TMS as a standard. MALDI-TOF mass spectra were recorded on a Micromass TofSpec 2E. The spectra were taken in reflectron mode at an accelerating voltage of +20 kV.

pH calibration curves were obtained in a microplate reader (FluoStar Optima, BMG Labtech, www.bmglabtech.com). The "cocktail" containing dissolved polymer (5% *w*/*w* THF or EtOH/H_2O mixtures) and dye (0.0125% *w*/*w*) was pipetted into 96-well polypropylene microtitreplates (Greiner Bio-one, www.gbo.com) and the solvent was allowed to evaporate. The obtained spots were incubated in the buffer solutions and interrogated using bandpass filters (475–490 nm for excitation, 585–600 nm for the PMT detector). The pH of the phosphate and acetate buffer solutions was controlled by a digital pH metre (InoLab pH/ion, WTW GmbH & Co. KG, www.wtw.com) calibrated at 25 °C with standard buffers of pH 7.0 and 4.0 (WTW GmbH & Co. KG, www.wtw.com). The buffers were adjusted to constant ionic strength using sodium chloride as the background electrolyte.

Sensor response curves were recorded with a two-phase lock-in amplifier (SR830, Stanford Research Inc., www.thinksrs.com) equipped with a blue LED (λ_{max} 455 nm) from Roithner (www.roithner-laser.com), a BG-12 short pass filter at the excitation side and a long-pass filter OG 550 (Schott, www.schott.com) before the PMT tube (H5701-02, Hamamatsu, www.sales.hamamatsu.com). The modulation frequency of 160 Hz was used.

For leaching tests, sensor foils (D4) were placed in a flow-through cell and the absorption of the films was monitored while aqueous buffers (ionic strength (IS), 100 mM) were passed through it.

Photobleaching experiments were performed by irradiating the samples with the light of a 458-nm high-power 10 W LED array (www.led-tech.de) focused through a lens purchased from Edmund optics (www.edmundoptics.de). Prior to the experiment a piece of the sensor foil (D4) was positioned in a quartz cuvette filled with the appropriate buffer. The photodegradation profiles were obtained by monitoring the absorption spectra. The absorption of the

sensing layers and in the maximum of the light source was adjusted to 0.1.

Calibration

The following sigmoidal function was used for sensor calibration:

$$I = \frac{A_{\min} - A_{\max}}{1 + e^{(pH - pK_a)/dx}} + A_{\max}, \quad (1)$$

where I is fluorescence intensity, $A_{\max}$, $A_{\min}$, and dx are numerical coefficients.

Results and discussion

Syntheses

As was mentioned above, PBIs belong to photochemically robust molecules which possess high fluorescence brightness. However, solubility of many perylene derivatives is often rather low [35]. The commercially available 1,6,7,12-tetrachloroperylene-3,4,9,10-tetracarboxylic bisanhydride (Fig. 2) was chosen as a starting material since the chloro substituents in the bay position remarkably increase solubility compared with unsubstituted perylenes without significantly affecting spectral properties. The imide position was selected for attaching PET functionalities since spectral properties are usually not influenced by imide substituents due to nodes in the molecular orbitals located at the nitrogen atoms [52]. Preliminary experiments showed that symmetric tetrachloroperylene bisimides with two PET functionalities show excellent acid–base sensitivity in organic solvents, but application in a hydrogel matrix was compromised by severe leaching of the dicationic protonated form. Hence, it was envisioned that a single PET functionality is sufficient to render the molecule pH sensitive whereas the second position can be occupied by a solubilising group which enhances solubility and provides sufficient lipophilicity. Among such groups the bulky 2,6-diisopropylphenyl moiety is known to significantly enhance the solubility of perylene dyes and is present in highly soluble commercial Lumogen® Red dye. Several diamines were utilized for introducing the PET functionality, including aliphatic and aromatic ones (Fig. 2).

It was found that **1** can be reacted with aliphatic amines under mild conditions but reaction with aromatic amines requires elevated temperature and acidic catalysis. Notably, asymmetric PBIs are often prepared via a monoanhydride monoimide as an intermediate [53, 54]. In the present case, however, this route is unpromising owing to poor stability of **1a** under the basic conditions that are usually employed for the preparation of the mentioned intermediate. The substantially different reactivities of aliphatic and aromatic amines did not allow simple coupling of an equimolar mixture with **1** (according to [55], for instance), but this concept was successfully employed for the preparation of bisaromatic compound **2d**. The indicators **2a–c** were prepared in a one-pot synthesis without isolation of the intermediate. Here, the second amine was added to the

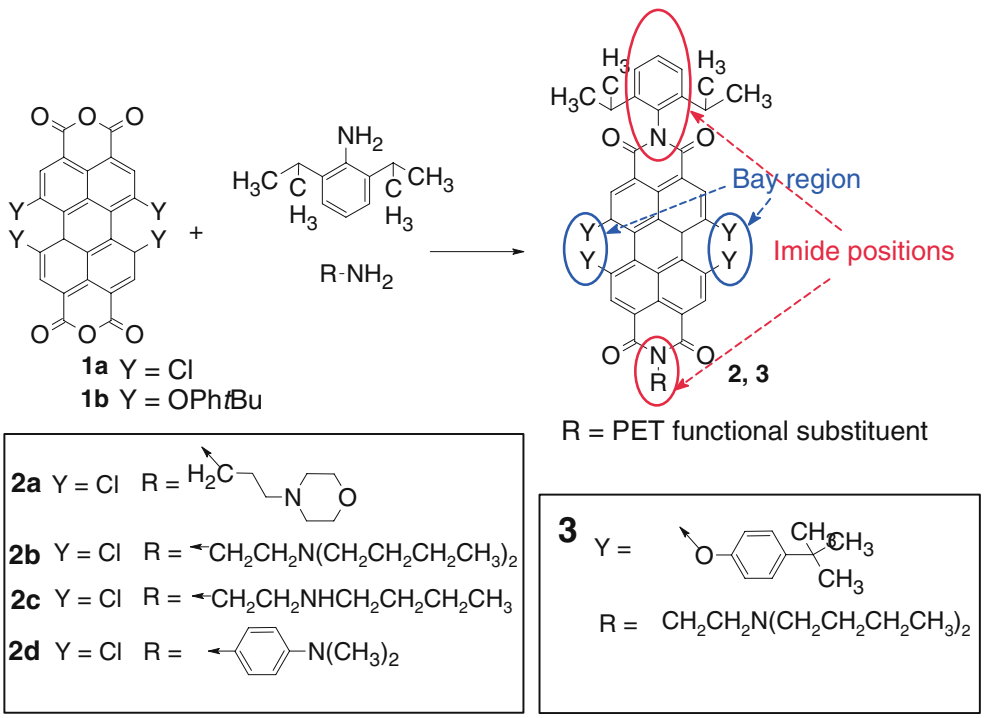

Fig. 2 Reagents and conditions: **2a**, **2b**: (1) R-NH_2 (1Eq.), NMP, 35 °C, 2 h; (2) 2,6-diisopropylaniline (4 eq), NMP/EtCOOH (4:1), 130 °C, 18 h; *2c*: (1) 2,6-diisopropylaniline (1.1 eq), NMP/EtCOOH (4:1), 130 °C, 18 h; (2) R-NH_2 (0.9 eq), 35 °C; *2d*: R-NH_2 (0.9 eq), 2,6-diisopropylaniline (1.1 eq), NMP, 130 °C, 24 h; *3:* (1) 2,6-diisopropylaniline (3 eq), NMP/EtCOOH (1:1), 130 °C, 24 h; (2) R-NH_2 (2 eq), 40 °C

reaction mixture after the reaction with the first amine was completed. The mixture of the asymmetric PBI and both symmetric PBIs was separable by column chromatography. The same concept was successfully employed also for the preparation of **3** starting from commercially available **1b**. The modest overall yields (7–36%) are explained by the formation of symmetric side products, naturally competing with the formation of the desired product. Nevertheless, all the products could be obtained in sufficient amount starting from reactants readily available at low cost.

Photophysical properties

Table 1 provides an overview of photophysical properties of the new indicators. They possess good luminescence brightnesses BS. The molar absorption coefficients ε are found to be ~40,000 M^{-1} cm^{-1} for all the indicators and the fluorescence quantum yields exceed 0.75. BS higher than 34,000 are obtained for all the dyes. These values are significantly higher than for the most common PET indicators based on naphthalimides (BS ~12,000). As expected, substitution of the chlorine atoms by 4-*tert*-butylphenoxy group results in a pronounced bathochromic shift of the absorption and emission bands. Note the very similar spectral properties of **2a–d** which indicates extensive decoupling between the chromophore and the amino-functional substituent.

Sensing properties in solutions

As expected, all the indicators possess much lower fluorescence quantum yields in the basic form compared with the acidic form (Table 1). Table 2 shows the solvent dependency of the acid/base sensitivity for **2b** and **3** as representative examples. Efficient PET effect (I_{acidic}/I_{bassic}> 10) is observable in all the solvents tested, with only minor influence of solvent polarity on PET efficiency and without a clear trend being recognizable. It should be mentioned here that the efficiency of a PET process can correlate with solvent polarity. For instance, for anthracence derivatives it was found to increase with polarity [56].

Table 2 PET efficiency of **2b** (8.10^{-8} M) and **3** (3.10^{-8} M) in organic solvents, expressed as the ratio between fluorescence intensity in acidic (CF_3COOH, 0.05% *v*/*v*) and basic (ethyldiisopropylamine, 0.05% *v*/*v*) solvent

Solvent	Dielectric constant	PET-efficiency	
		2b	**3**
n-Hexane	1.9	41	1.9
Toluene	2.4	62	3.9
Methyl *tert*-butyl ether	2.6	42	3.5
Chloroform	4.7	47	4.6
Ethyl acetate	6.0	43	5.6
Tetrahydrofuran	7.4	42	5.5
Acetone	20	43	4.6
1-Propanol	20	32	4.6
Ethanol	24	39	4.9
Methanol	33	27	3.9

Sensing properties in polymeric films

The pH sensors were obtained by non-covalently entrapping the indicators into hydrogels. D4 (a polyurethane hydrogel), poly(hydroxypropylmethacrylate) and poly(hydroxyethylmethacrylate) were used. Immobilization has little effect on the absorption and the emission spectra of the indicators which shift bathochromically. For example, the absorption and emission in D4 were found to peak at 525 and 558 nm, respectively, for **2a**, and at 589 and 622 nm, respectively, for **3**. The sensing layers obtained show bright fluorescence which is visible with the naked eye at daylight. It should be mentioned that fluorescence of **3** in poly(hydroxyalkylmethacrylates) is weak which is likely to be caused by aggregation of the indicator. In agreement to the behaviour expected for a PET sensor, the fluorescence excitation and emission spectra are diminished in intensity but not altered in shape as pH is increased (Fig. 3). The absorption spectra remain almost unaltered and their pH-dependent spectral shift does not exceed 5 nm in all cases. Such behaviour was found for all PBIs presented. As expected, fluorescence intensities of the indicators show typical sigmoidal shapes of

Table 1 Photophysical properties of the perylene bisimide indicators in solution

Dye	λ_{max} abs($\varepsilon \cdot 10^{-4}$)/nm ($M^{-1} \cdot cm^{-1}$) CH_2Cl_2	λ_{max} em/nm CH_2Cl_2	QY acidic $CHCl_3$	QY basic $CHCl_3$
2a	520 (3.98); 486 (2.76); 427 (1.05)	552	0.95	0.044
2b	520 (4.00); 486 (2.78); 426 (1.04)	552	0.95	0.015
2c	521 (4.13); 487 (2.88); 427 (1.11)	554	0.84	0.055
2d	520 (4.54); 487 (3.16); 426 (1.18)	559	0.81	<0.001
3	582 (4.45); 542 (2.70); 452 (1.62)	624	0.76	0.11

Since pH-induced spectral shifts are small (<5 nm in all cases), maxima are reported for acidic media only

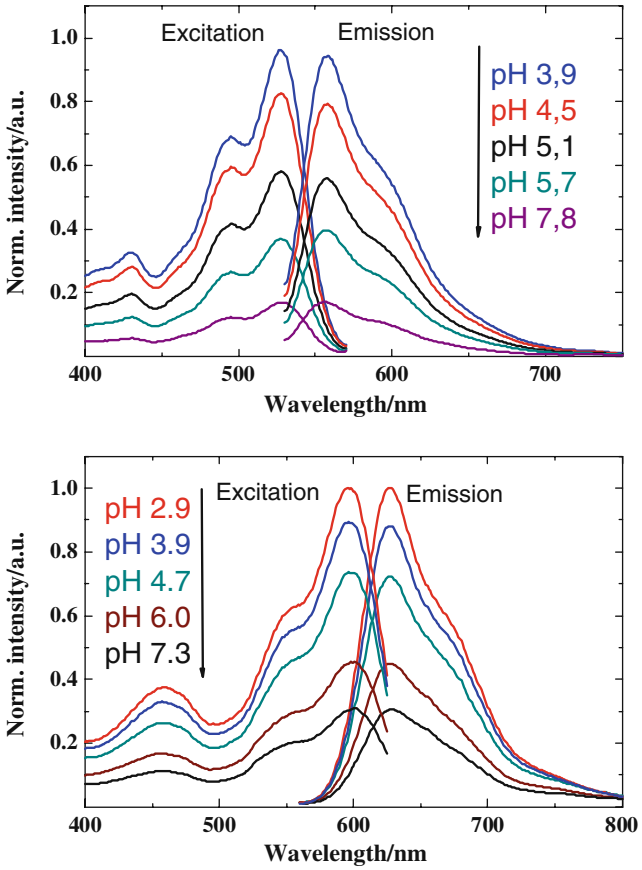

Fig. 3 pH-dependent optical properties of **2a** (*top*) and **3** (*bottom*) in hydrogel D4; IS=100 mM. Fluorescence excitation spectra were acquired at λ_{em}=580 nm and 640 nm, fluorescence emission was excited at 515 and 550 nm for **2a** and **3**, respectively

the calibration plots (Fig. 4) from which the apparent pK_a values can be obtained. The apparent pK_a values as well as the intensity ratios for the acidic and the basic form of the dye are summarized in Table 3.

Table 3 demonstrates that the apparent pK_a values can be tuned by introducing amino groups with different basic character. The acidity of the protonated form decreases in the order 2d>2a≈2b>2c which corresponds to the general trend expected for aromatic, tertiary and secondary amines. On the other hand, the apparent pK_a values are also influenced by the polymer matrix. Significantly higher pK_a values (9.5–10) were reported for comparable compounds in solution [49]. Localization in the less polar environment of the hydrogel matrix may decrease the apparent pK_a values since the charged acidic form is destabilized in these regions. This effect is opposite in case of anionic indicators (such as fluoresceins) which are known to have higher pK_a values in less polar environment. The generally higher pK_a values in pHPMA can be explained by higher hydrophilicity of the former compared with the hydrogel D4 which is a block copolymer containing both hydrophilic and hydrophobic domains. In this context, the pK_a values found in pHEMA are unexpectedly low, considering that pHEMA is even more polar than pHPMA. A possible explanation is partial aggregation of the lipophilc dyes in this relatively hydrophilic matrix. In fact, the brightness of pHEMA sensor films is lower than in the other polymer matrices which also suggests limited solubility of the dye in pHEMA.

It can be summarized that both the nature of the aminogroup and the polymer can be used to tune the dynamic

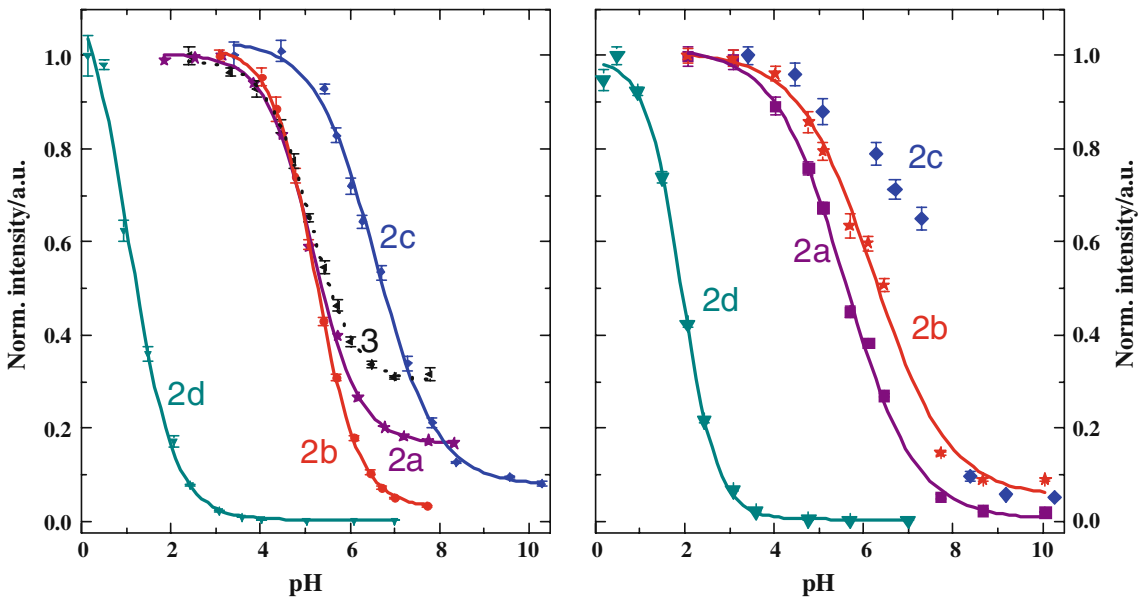

Fig. 4 Calibration curves for the PBI indicators. *Left*, in D4 hydrogel; *right*, in poly(hyroxypropylmethacrylate). In poly(hyroxypropylmethacrylate), **2c** does not show a typical sigmoidal calibration curve, therefore the apparent pK_a was not determined. Since **3** shows only weak fluorescence in the same matrix, the corresponding calibration curve is not displayed

Table 3 Calibration parameters of the indicators in hydrogels D4, poly(hydroxypropylmethacrylate) (pHPMA) and poly (hydroxyethylmethacrylate) (pHEMA): apparent pK_a values and the PET efficiency defined as the intensity ratio for the acidic and the basic forms of the indicator I_A/I_B

Dye	Matrix					
	D4		pHPMA		pHEMA	
	Apparent pK_a	I_A/I_B	Apparent pK_a	I_A/I_B	Apparent pK_a	I_A/I_B
2a	5.1	5.5	5.6	47	4.9	26
2b	5.2	29	6.2	13	4.8	28
2c	6.5	12	–	8.6	6.8	38
2d	1.1	$4{\cdot}10^3$	1.9	$7{\cdot}10^3$	–	–
3	5.1	3.3	–	–	–	–

range of the sensor. Notably, the pK_a values obtained for **2b** and **3** are very similar despite their significantly different spectral properties. Therefore, the concept is likely to be transferable to other perylene-based indicators with different spectral properties. In terms of the dynamic range the sensors presented here are adequate for biotechnological applications. However, the pK_a values are generally too low for the sensors to be suitable for measurements at physiological conditions and in seawater. On the other hand, the indicator bearing an aromatic amine (**2d**) may find application for monitoring pH in strongly acidic media.

The PET efficiencies (defined as the ratio of the fluorescence intensities for the acidic I_A and the basic forms I_B of the indicator) are also collected in Table 3. Generally, Weller's equation [57] can be used to predict the PET efficiency [14, 49] if the redox potentials of the fluorophore and the quencher are known:

$$\Delta G_{PET} = E^{ox}_{Rec} - E^{Red}_{Fluo} - E^{S}_{Fluo} - E_{Ion} \quad (2)$$

where ΔG is the thermodynamic driving force for PET, E^{Ox}_{Rec}, E^{Red}_{Fluo} are the oxidation/reduction potentials of amino function and fluorophore, respectively, E^{S}_{Fluo} is the energy of the singlet excited state of the fluorophore, and E_{Ion} is the ion pairing energy of the PET products.

As can be seen, the highest PET efficiency is observed for the aromatic amine (which is "switched off" in the basic form) and it is lower for the aliphatic amines. The sensitivity of **3** is significantly reduced compared with **2b** which bears the same PET functionality. The replacement of electron-withdrawing chlorine atoms by electron-donating aryloxy groups is expected to decrease the thermodynamic driving force for PET since (1) electron density in the chromophore is increased and its reduction, therefore, becomes less favourable and (2) E^{S}_{Fluo} decreases since **3** is excited at longer wavelength than **2b**. Nevertheless, a value of 3.3 still is sufficient for effective sensing. However, the above trend should be considered if bathocromically shifted pH indicators are designed since the PET efficiency may become too low for practical applications.

pH sensor with enlarged dynamic range

As was demonstrated above the spectral properties of the indicators **2a–d** are virtually identical (Table 1) which provides the possibility of designing a pH sensor with enlarged dynamic range. To demonstrate the feasibility of the approach **2b** and **2c** were mixed together in the same sensor material. The absorption and the emission spectra of the hybrid material are virtually identical to the spectra of the individual probes (Fig. 5). The response of the sensor is also shown in Fig. 5. Indeed, the dynamic range of the new

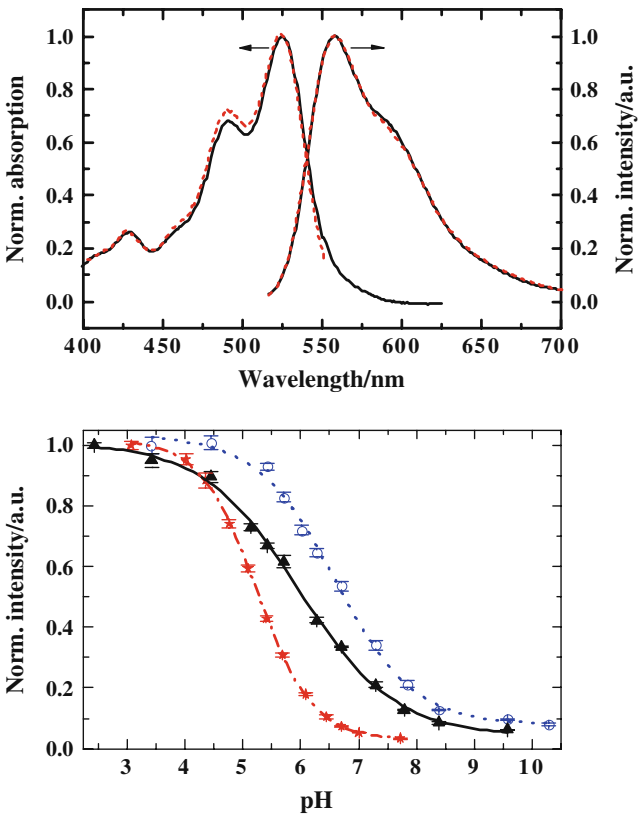

Fig. 5 Characteristics of the broadband pH sensor containing **2b** (0.08% *w/w*) and **2c** (0.16% *w/w*) in hydrogel D4: *Top*, spectral properties of the sensor (*thick black line*) compared with those of **2b** (*thin red line*); *bottom*, the respective calibration curves (*triangles* broadband sensor, *stars* **2b**, and *circles* **2c**). Conditions: IS=100 mM, RT

sensor is extended by ~2 units compared with the sensors based on single indicators. The calibration curve can still be fitted with Eq. 1 (correlation coefficient, >0.998). In the same way, **2b** can be combined with **2d.** Since the pK_a values of both differ significantly, a two-step pH response is obtained (Fig. S1 in the Electronic supplementary material). It should be emphasized here that the functionalities determining the pK_a value have very little influence on spectral and photophysical properties of the PBI indicators. Undesired effects caused by inner filter effects, Förster Resonance Energy Transfer between the probes or unlike photostabilities are therefore minimized. This is in contrast to other classes of pH indicators (e.g. fluoresceins) where the design of a broadband sensor is compromised by such effects. On the contrary, the PBI indicators presented here seem to be ideally suitable for the design of a broadband sensor. Such a sensor may represent an alternative to a glass electrode in various applications (e.g. environmental monitoring).

Cross-sensitivity to ionic strength

Cross-sensitivity to IS is a common drawback of optical pH sensors. The effect of the ionic strength on the calibration plots can be rather small if the charge of the indicator is minimal. In fact, the lipophilic fluorescein derivatives (neutral in the protonated form and bearing a single negative charge in the deprotonated form) were demonstrated to possess very low cross-sensitivity to IS [1]. Figure 6 shows the response of a pH sensor based on an individual PBI (dye **3** in hydrogel D4) and the response of the broadband sensor based on the mixture of **2b** and **2c**. Evidently, both sensors exhibit virtually negligible cross-sensitivity to IS. In fact, the alteration of the IS from 50 to 500 mM is accompanied by the increase of the apparent pK_a values by ≈0.1 units.

Leaching tests

In case of **2a**, **2b**, **2d** and **3**, no leaching into the aqueous solution is detectable after 24 h in basic ($pH > pK_A + 2$) and acidic buffers ($pH < pK_A - 2$) which is in contrast to severe leaching observed for the indicators bearing two PET functionalities. In case of **2c** in D4, the absorption decreased by 7% within the first 6 h at acidic pH but slowed after that (0.2%/h). No decrease was observed in basic buffer. Consequently, leaching is not critical for the investigated sensors due to pronounced hydrophobicity of the indicator dyes.

Photostability

Figure 7 demonstrates the photodegradation profiles for three pH indicators, namely perylene-based **2b** and **3**, and fluorescein octadecyl ester (FODE) which is used for comparison. Surprisingly, the photostability of the tetrachloro-PBI indicators **2a**–**d** was found to be rather poor. In fact, the dyes bleach even faster than FODE. The rapid photodegradation is accompanied by the formation of

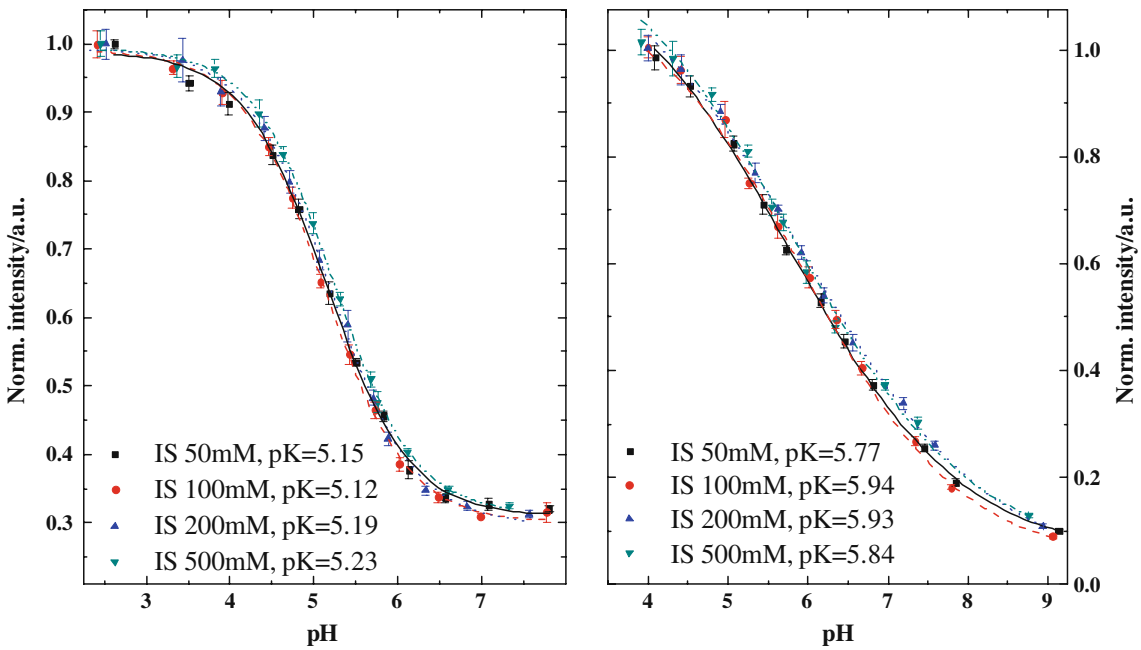

Fig. 6 Ionic strength dependency of the calibration curves of the pH sensors. *Left*, for the sensor based on **3** (0.25% *w/w*) in D4; *right*, for broadband sensor containing **2b** (0.08% *w/w*) and **2c** (0.16% *w/w*) in D4

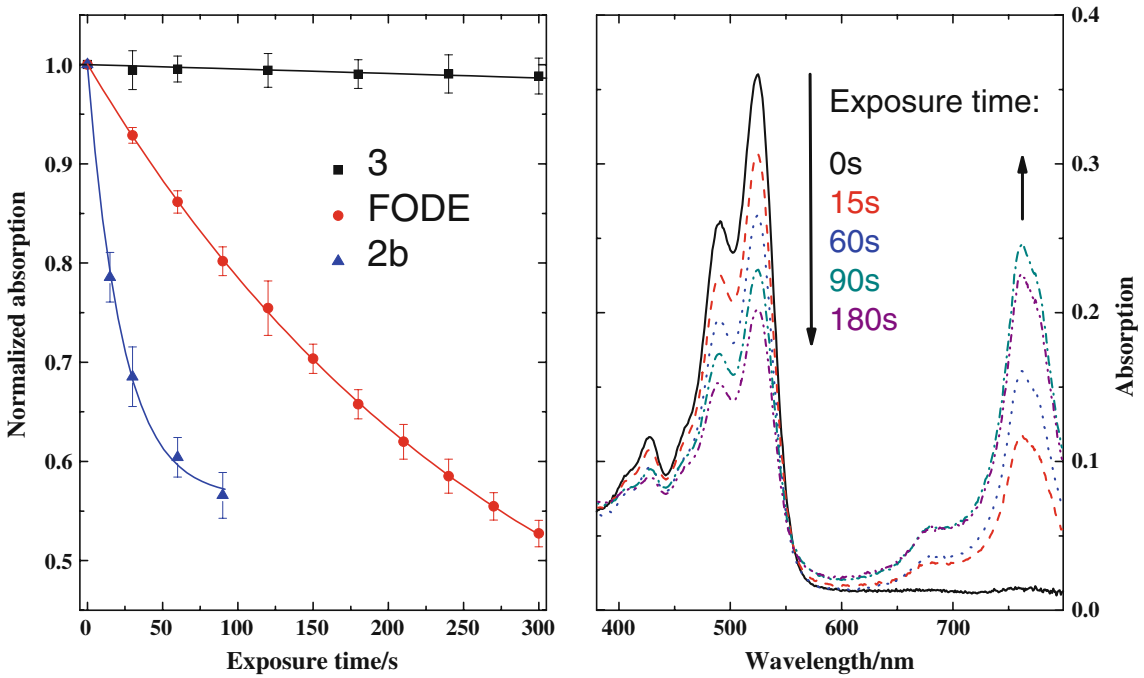

Fig. 7 Photobleaching of perylene bisimide indicators in hydrogel D4. *Left*, decrease in absorption for tetrachloro-substituted PBI **2b** and tetraaryloxy-substituted PBI **3**, and for fluorescein octadecyl ester (*FODE*); *right*, spectral changes accompanying the decomposition of **2b**

a new dye which absorbs in NIR (700–800 nm, Fig. 7, right). One of the possible bleaching pathways may be substitution of the chlorine atoms by hydroxide ions or water. This assumption is supported by the fact that the photostability of dissolved **2a**–**d** deteriorates in the presence of water, but it improves significantly in organic solvents such as tetrahydrofurane (THF). If water is added to THF the bleaching rate increases proportionally. Interestingly, the bleaching reaction is accompanied by an increase of fluorescence in unbuffered organic solvents which suggests the formation of HCl. The photobleaching rate of 1,6,7,12-tetrachloro-*N,N′*-(2,6-diisopropylphenylperylene-3,4,9,10-tertracarboxylic bisimide which bears no PET functionality was found to be similar which also suggests that the photobleaching pathway is determined by the presence of the halogens rather than the presence of a PET functionality.

It is evident that substitution of the chlorine atoms in the PBI molecule by aryloxy groups renders the molecule highly photostable (Fig. 7, left). In fact, bleaching for **3** is several orders of magnitude slower than for FODE. For example, FODE degraded by almost 50% after 5 min of irradiation whereas 3 h of irradiation of **3** results in degradation of only 1.5% (pH 1.5) or 3% of the indicator (pH 9.6). Notably, the phototostability of **3** in organic solvent is not affected by the presence of water. Evidently, the aryloxy-substituted PBI is a platform of choice for designing pH sensors, but the tetrachloro-substituted derivatives are excluded from many applications due to their poor photostability.

Dynamic response

Figure 8 demonstrates the response of the sensor based on **2b** in hydrogel D4 to an alteration of pH. As can be seen, the response is reversible and fairly fast (t_{90} is 5 min on going from pH 6 to 4.3 and <30 s in the reverse direction). The response time is a critical parameter if pHPMA is used as immobilization matrix. Significantly longer response times (>1 h) are characteristic even for the thin (2 μm) sensing layers. In contrast to that, the sensors based on pHEMA are found to have significantly faster response which is comparable to the D4-based sensors. Generally,

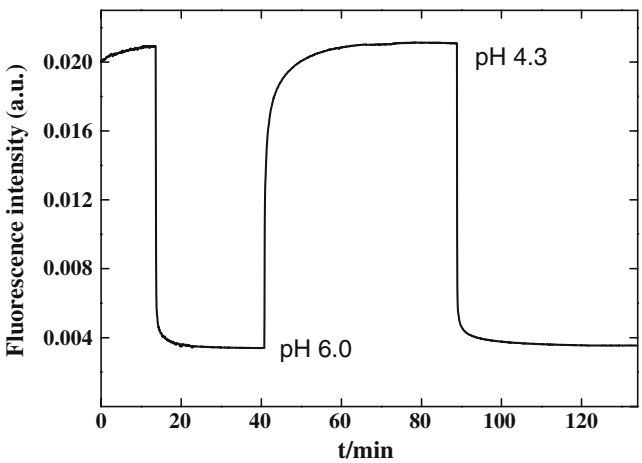

Fig. 8 Response curves of **2b** in D4 (dye content 1%, layer thickness 5 μm) to dynamic changes of pH

the sensors respond considerably faster to increasing pH than to its decreasing.

It was found that the sensors based on **3** embedded in hydrogel D4 respond much slower than the sensors based on **2a–d**. In freshly prepared foils, t_{90} can be ~10 min on going from pH 6 to 4 and ~5 min in the reverse direction. However, a considerable flattening of the curve causes significantly longer t_{95} (~60 and 15 min, respectively). It should also be noted that response times tend to significantly increase over storage time. That also results in worse reversibility for older foils. Evidently, very long response times for **3** indicate its localization in hydrophobic domains of the hydrogel. Several strategies can be proposed for improving the response times of the indicators. For example, significantly less hydrophobic aryloxy substituents can be used to force the indicator into more hydrophilic regions. Covalent immobilization (for instance via replacement of the 2,6-diisopropylphenyl substituent with a vinyl or acrylate moiety and subsequent co-polymerization) may also help to provide a hydrophilic environment for the indicator.

Long-term stability

In hydrogel D4, the calibration curves show some drift towards lower I_A/I_B if the sensors are stored in buffer solution for several days (Fig. 9). For instance, in case of **2a**, I_A/I_B decreases from 5.5 to 2.9 within 4 weeks. Notably, the apparent pK_a values remain constant. Slow aggregation of the indicator is a possible reason for this phenomenon. Nevertheless, the drift is negligible within an interval of a few hours, but for longer measurements recalibration is required. On the other hand, virtually no drift was observed for the sensors based on pHPMA. Those sensors can be used for weeks without considerably changing their calibration plots.

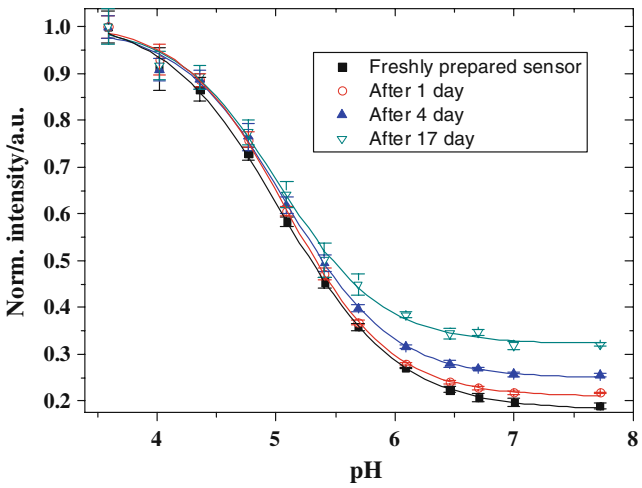

Fig. 9 Calibration plots for **2a** (0.25% *w*/*w*) in D4 followed over time. The sensors were stored in aqueous buffers (IS=100 mM) in the darkness

Referencing

Evidently, fluorescence intensity is a rather ambitious parameter which is affected by various factors such as light intensity of the excitation source, sensitivity of the detector, turbidity of the probe etc. Therefore, different referencing schemes are commonly employed. For the sensors presented above ratiometric measurements become possible by immobilizing a fluorescent pH-insensitive dye in the same matrix (Fig. S2 in the Electronic supplementary material). Other schemes such as Dual Lifetime Referencing are also possible.

Conclusions

pH-sensitive PET functional perylene bisimides (PBIs) were obtained in a single reaction step starting from commercially available compounds. The new indicators possess good luminescence brightness which is substantially higher that for common PET indicators such as naphthalimides. Two classes of PBIs with differing spectral properties were investigated: tetrachloro-PBIs (**2a**–**d**) and a tetra-aryloxyPBIs (**3**) which features bathochromically shifted absorption and emission spectra. Due to their small charge the sensing materials possess virtually negligible cross-sensitivity to ionic strength. The sensors based on tetrachloro-PBIs possess good brightness in hydrogels D4, pHPMA and pHEMA and show excellent PET efficiencies. The pK_a value of the sensor can be tuned by attaching different amino groups to the PBI indicator. Virtually identical photophysical properties allow the preparation of a sensor for a broad pH range (>4 pH units). Unfortunately, the sensors based on tetrachloro-PBIs photodegradate readily. On the contrary, those based on the tetra-aryloxy-substituted **3** possess unmatched photostability which is orders of magnitude higher than that of a common fluorescein-based indicator. As is demonstrated, the pK_a value is not considerably influenced by the nature of the chromophore. This suggests that tunability of pK_a is applicable to tetra-aryloxy-substituted PBIs and other perylene chromophores. The performance of the sensor based on **3** is compromised by long dynamic response which indicates localization of the indicator in the hydrophobic domains of the hydrogel. It can be concluded that the PET-based perylenes represent a promising class of pH indicators featuring excellent brightnesses, high photostabilities and tunability of proton affinity and spectral properties. They constitute a platform for the future design

of high-performance pH sensors that may outperform existing systems. However, all presented sensors still suffer from drawbacks. The poor photostability of those based on tetrachloro-PBIs has been shown to be outstandingly improved by using tetra-aryloxy-substituted **3**. To overcome the issues of slow dynamic response and signal drifts, optimization in the indicator structure or/and covalent immobilization into the polymer network are the most promising concepts.

Acknowledgements The financial support from the Austrian Science Fund FWF (project P 21192-N17) is gratefully acknowledged. We thank Prof. Robert Saf (Graz University of Technology) for acquiring MS spectra.

References

1. Weidgans BM, Krause C, Klimant I, Wolfbeis OS (2004) Analyst 129:645–650
2. Allard E, Larpent C (2008) J polym sci polym chem 46:6206–6213
3. McNamara KP, Nguyen T, Dumitrascu G, Ji J, Rosenzweig N, Rosenzweig Z (2001) Anal Chem 73:3240–3246
4. Strömberg N, Mattsson E, Hakonen A (2009) Anal Chim Acta 636:89–94
5. Schulman SG, Shangxian Chen, Bai F, Leiner MJP, Weis L, Wolfbeis OS (1995) Anal Chem 304:165–170
6. Borisov SM, Herrod DL, Klimant I (2009) Sensor Actuator B Chem 139:52–58
7. Opitz N, Lübbers D (1983) Sensor Actuator 4:473–479
8. Grant SA, Glass RS (1997) Sensor Actuator B Chem 45:35–42
9. Parker JW, Laksin O, Yu C, Lau ML, Klima S, Fisher R, Scott I, Atwater BW (1993) Anal Chem 65:2329–2334
10. Xu Z, Rollins A, Alcala R, Marchant RE (1998) J Biomed Mater Res 39:9–15
11. Kuwana E, Liang F, Sevick-Muraca E (2004) Biotechnol Prog 20:1561–1566
12. Whitaker JE, Haugland RP, Prendergast FG (1991) Anal Biochem 194:330–344
13. Borisov SM, Gatterer K, Klimant I (2010) Analyst 135:1711
14. Bissell RA, Silva APD, Gunaratne HQN, Lynch PLM, Maguire GEM, Sandanayake KRAS (1992) Chem Soc Rev 21:187–195
15. Bissell RA, Calle E, Silva APD, Silva SAD, Gunaratne HQN, Habib-Jiwan J, Peiris SLA, Rupasinghe RADD, Shantha TK, Samarasinghe D, Sandanayake KRAS, Soumillion J (1992) J Chem Soc Perkin trans 2:1559–1564
16. Brown GJ, Silva APD, James MR, McKinney BOF, Pears DA, Weir SM (2008) Tetrahedron 64:8301–8306
17. Kubo K, Mori A (2005) J Mater Chem 15:2902
18. Mes GF, Van Ramesdonk HJ, Verhoeven JW (1984) J Am Chem Soc 106:1335–1340
19. Silva APD, Rupasinghe RADD (1985) J Chem Soc Chem Commun 1669–1670
20. Saleh N, Al-Soud YA, Nau WM (2008) Spectrochim acta Mol spectrosc 71:818–822
21. Li Z, Niu C, Zeng G, Liu Y, Gao P, Huang G, Mao Y (2006) Sensor Actuator B Chem 114:308–31
22. Tian Y, Su F, Weber W, Nandakumar V, Shumway BR, Jin Y, Zhou X, Holl MR, Johnson RH, Meldrum DR (2010) Biomaterials 31:7411–7422
23. Trupp S, Hoffmann P, Henkel T, Mohr GJ (2008) Org Biomol Chem 6:4319
24. Niu C, Zeng G, Chen L, Shen G, Yu R (2004) Analyst 129:20–24
25. Hirano T, Kikuchi K, Urano Y, Higuchi T, Nagano T (2000) Angew Chem Int Ed 39:1052–1054
26. Golchini K, Mackovic-Basic M, Gharib SA, Masilamani D, Lucas ME, Kurtz I (1990) Am J Phys 258:438–443
27. Silva APD, Sandanayake KRAS (1989) J Chem Soc Chem Commun 1183–1185
28. Silva APD, Gunaratne HQN (1990) J Chem Soc Chem Commun 186–188
29. Pearson AJ, Xiao W (2003) J Org Chem 68:5369–5376
30. Zhang Z, Wu D, Guo X, Qian X, Lu Z, Xu Q, Yang Y, Duan L, He Y, Feng Z (2005) Chem Res Toxicol 18:1814–1820
31. Lee JH, Jeong AR, Shin I, Kim H, Hong J (2010) Org Lett 12:764–767
32. Silva APD, Gunnlaugsson T, Rice TE (1996) Analyst 121:1759–1762
33. Kohl C, Weil T, Qu J, Müllen K (2004) Chem Eur J 10:5297–5310
34. Langhals H, Ismael R, Yürük O (2000) Tetrahedron 56:5435–5441
35. Seybold G, Wagenblast G (1989) Dyes Pigm 11:303–317
36. Rademacher A, Märkle S, Langhals H (1982) Chem Ber 115:2927–2934
37. Chiu T, Chuang K, Lin C, Ho Y, Lee J, Chao C, Leung M, Wan D, Li C, Chen H (2009) Thin Solid Films 517:3712–3716
38. Breeze AJ, Salomon A, Ginley DS, Gregg BA, Tillmann H, Horhold H (2002) Appl Phys Lett 81:3085–3087
39. Reisfeld R, Yariv E, Minti H (1997) Opt Mater 8:31–36
40. Wurthner F, Stepanenko V, Chen Z, Saha-Moller CR, Kocher N, Stalke D (2004) J Org Chem 69:7933–7939
41. Fan L, Xu Y, Tian H (2005) Tetrahedron Lett 46:4443–4447
42. Qiu W, Chen S, Sun X, Liu Y, Zhu D (2006) Org Lett 8:867–870
43. Rehm S, Stepanenko V, Zhang X, Rehm T, Würthner F (2010) Chem Eur J 16:3372–3382
44. Schnurpfeil G, Stark J, Wöhrle D (1995) Dyes Pigm 27:339–350
45. Avlasevich Y, Li C, Mullen K (2010) J Mater Chem 20:3814–3826
46. Avlasevich Y, Müller S, Erk P, Müllen K (2007) Chem Eur J 13:6555–6561
47. Weil T, Abdalla MA, Jatzke C, Hengstler J, Mullen K (2005) Biomacromolecules 6:68–79
48. Ren T, Mandal PK, Erker W, Liu Z, Avlasevich Y, Puhl L, Müllen K, Basché T (2008) J Am Chem Soc 130:17242–17243
49. Daffy LM, Silva APD, Gunaratne HQN, Huber C, Lynch PLM, Werner T, Wolfbeis OS (1998) Chem Eur J 4:1810–1815
50. Langhals H, Pust T (2010) Z Naturforsch 65:291–294
51. Wang E, Wang G, Ma L, Stivanello CM, Lam S, Patel H (1996) Anal Chim Acta 334:139–147
52. Langhals H, Demmig S, Huber H (1988) Spectrochim Acta Mol Spectros 44:1189–1193
53. Kaiser H, Lindner J, Langhals H (1991) Chem Ber 124:529–535
54. Tröster H (1983) Dyes Pigm 4:171–177
55. Baffreau J, Leroy-Lhez S, Vân Anh N, Williams R, Hudhomme P (2008) Chem Eur J 14:4974–4992
56. Bissell RA, de Silva AP, Thilak W, Fernando ML, Patuwathavithana ST, Shantha TK, Samarasinghe D (1991) Tetrahedron Lett 32:425–428
57. Weller A (1968) Pure Appl Chem 16:115–124